Inorg. Chem. **2004**, *43*, 1638–1648

Spectroscopic and Electrochemical Characterization of an Aqua Ligand Exchange and Oxidatively Induced Deprotonation in Diiron Complexes

Sylvie Chardon-Noblat,[†] Olivier Horner,[‡] Barbara Chabut,[‡] Frédéric Avenier,[‡] Noëlle Debaecker,[‡] Peter Jones,[‡] Jacques Pécaut,[§] Lionel Dubois,[‡] Claudine Jeandey,[‡] Jean-Louis Oddou,[‡] Alain Deronzier,[†] and Jean-Marc Latour*[,‡]

Laboratoire d'Electrochimie Organique et de Photochimie Rédox, UMR CNRS 5630, ICMG FR CNRS 2607, Université Joseph Fourier Grenoble 1, BP 53, 38041 Grenoble Cédex 9, France, CEA-Département de Recherche Fondamentale sur la Matière Condensée, Service de Chimie Inorganique et Biologique, UMR CEA-CNRS-UJF 5630, Laboratoire des Métalloprotéines, UMR CEA-CNRS-UJF 5046, CEA/Grenoble, 38054 Grenoble Cédex 9, France, and CEA-Département Réponse et Dynamique Cellulaires, Laboratoire de Physicochimie des Métaux en Biologie, FRE CEA-CNRS-UJF 2427, CEA/Grenoble, 38054 Grenoble Cédex 9, France

Received June 10, 2003

Reaction of the unsymmetrical phenol ligand 2-((bis(2-pyridylmethyl)amino)methyl)-6-(((2-pyridylmethyl)benzylamino)-methyl)-4-methylphenol (HL-Bn) or its 2,6-dichlorobenzyl analogue (HL-BnCl$_2$) with Fe(H$_2$O)$_6$(ClO$_4$)$_2$ in the presence of disodium *m*-phenylenedipropionate (Na$_2$(mpdp)) followed by exposure to atmosphere affords the diiron(II,III) complexes [Fe$_2$(L-Bn)(mpdp)(H$_2$O)](ClO$_4$)$_2$ and [Fe$_2$(L-BnCl$_2$)(mpdp)(CH$_3$OH)](ClO$_4$)$_2$, respectively. The latter complex has been characterized by X-ray crystallography. It crystallizes in the monoclinic system, space group $P2_1/n$, with $a = 13.3095(14)$ Å, $b = 20.1073(19)$ Å, $c = 19.4997(19)$ Å, $\alpha = 90°$, $\beta = 94.471(2)°$, $\gamma = 90°$, $V = 5202.6(9)$ Å^3, and $Z = 4$. The structure of the compound is very similar to that of [Fe$_2$(L-Bn)(mpdp)(H$_2$O)](BPh$_4$)$_2$ determined earlier, except for the replacement of a water by a methanol on the ferrous site. Magnetic measurements of [Fe$_2$(L-Bn)(mpdp)(H$_2$O)](BPh$_4$)$_2$ reveal that the two high-spin Fe ions are moderately antiferromagnetically coupled ($J = -3.2(2)$ cm^{-1}). Upon dissolution in acetonitrile the terminal ligand on the ferrous site is replaced by a solvent molecule. The acetonitrile–water exchange has been investigated by various spectroscopic techniques (UV–visible, NMR, Mössbauer) and electrochemistry. The substitution of acetonitrile by water is clearly evidenced by Mössbauer spectroscopy by a reduction of the quadrupole splitting value from 3.14 to 2.41 mm/s. In addition, it causes a 210 mV downshift of the oxidation potential of the ferrous site and a similar reduction of the stability domain of the mixed-valence state. Exhaustive electrolysis of a solution of [Fe$_2$(L-Bn)(mpdp)(H$_2$O)]$^{2+}$ shows that the aqua diferric species is not stable and undergoes a chemical reaction which can be partly reversed by reduction to the mixed-valent state. This and other electrochemical observations suggest that upon oxidation of the diiron center to the diferric state the aqua ligand is deprotonated to a hydroxo. This hypothesis is supported by Mössbauer spectroscopy. Indeed, this species possesses a large quadrupole splitting value ($\Delta E_Q \geq 1.0$ mm·s^{-1}) similar to that of analogous complexes with a terminal phenolate ligand. This study illustrates the drastic effects of aqua ligand exchange and deprotonation on the electronic structure and redox potentials of diiron centers.

Introduction

Hemerythrin (Hr) is a dioxygen carrier found in sipunculid worms and other marine invertebrates.[1] As the first structurally known protein with a dinuclear iron active site, it was long considered as the prototype of this class. However, subsequent structure resolutions of other proteins of the class have shown that instead it is rather an exception.[2] Since the

* To whom correspondence should be addressed. E-mail: jlatour@cea.fr.
† Université Joseph Fourier Grenoble 1.
‡ Laboratoire de Physicochimie des Métaux en Biologie, CEA/Grenoble.
§ Service de Chimie Inorganique et Biologique, CEA/Grenoble.

(1) Wilkins, P. C.; Wilkins, R. G. *Coord. Chem. Rev.* **1987**, *79*, 195−214.
(2) Kurtz, D. M. *JBIC* **1997**, *2*, 159−167.

10.1021/ic030192+ CCC: $27.50
Published on Web 02/05/2004

early 1980s, the structures of several Hr forms have been solved by X-ray crystallography.[3−5] The protein backbone furnishes the iron pair with five terminal histidines and two bridging carboxylates from an aspartate and a glutamate. In the deoxy form, the two Fe^{2+} ions are bridged by a hydroxide resulting in an asymmetric coordination: one iron is hexacoordinated with a N_3O_3 environment while the other one is only pentacoordinated with a N_2O_3 environment and possesses a vacant coordination site for dioxygen interaction.[3] Upon dioxygen binding, the diiron pair is oxidized to the diferric state while the hydroxide bridge is deprotonated. The resulting hydroperoxide is bound to the Fe^{3+} ion in the N_2O_3 site and forms a hydrogen bond with the oxo bridge. The hydroperoxo ligand of the oxy form can be replaced by anions (e.g. azide) leading to the corresponding met forms, which have been structurally characterized.[3−5]

Apart from the diferrous and diferric states, two mixed-valent [$Fe^{II}Fe^{III}$] semimet forms have been prepared in vitro, either by reduction of the met form (semimet$_R$ Hr) or by oxidation of the deoxy form (semimet$_O$ Hr). None of them has been structurally characterized by X-ray crystallography yet. Nevertheless, extensive spectroscopic studies have identified a [$Fe^{II}(\mu$-OH)Fe^{III}] unit[6,7] and shown that the two forms differ by the localization of the iron valences in the two distinct protein coordination sites: in semimet$_O$ Hr the Fe^{II} is in the N_2O_3 site and accessible to solvent molecules while in semimet$_R$ Hr the Fe^{III} occupies the N_2O_3 site and is bound by a hydroxide ion.[8,9]

(μ-Oxo)bis(μ-acetato)diiron(III) complexes of tridentate amine ligands (hydrotris(pyrazolyl)borate, triazacyclononane) were first developed as models of methemerythrins and indeed reproduced their physical properties.[10,11] Nevertheless, the terminal ligands saturated the iron coordination spheres and could not allow the binding of an exogeneous ligand. This was achieved by Wieghardt et al.[12] by combining a diamine and a triamine to bind the diiron core and more recently by Lippard et al. using 1,8-naphthyridine-based ligands[13] or diamines in conjunction with sterically encumbered dicarboxylates.[14] We used a different approach on the basis of an asymmetrical phenolato ligands to mimic the asymmetrical histidine coordination in Hr, the phenoxo bridge playing the role of the hydroxide.[15,16] The same approach was used by Balch, Satcher, et al.[17,18] with similar ligands providing the iron atoms with an alkoxo bridge.

Chart 1. Representation of (a) the Ligand HL-Bn (and Substituted Derivatives) and (b) the Cation $[Fe_2(L\text{-}Bn)(mpdp)(H_2O)]^{2+}$

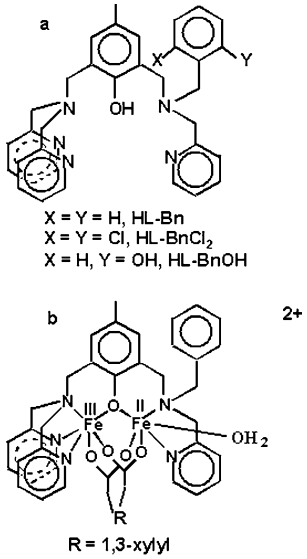

In the course of our studies, we used the asymmetrical hexadentate pentaamine ligand HL-Bn (Chart 1), which does not saturate the coordination of one iron of the pair. Indeed, its mixed-valent complex [Fe^{III}(L-Bn)(mpdp)$Fe^{II}(H_2O)$]-$(BPh_4)_2$, in which the two irons are bridged by the two carboxylate groups of 1,3-benzenedipropionate (mpdp), possesses a water molecule completing the coordination of the Fe^{2+} ion.[15] In this article, we report extensive spectroscopic and electrochemical studies of the exchange of this terminal aqua ligand. In addition, we report the X-ray structure of the methanol adduct of the mixed-valent complex of a similar ligand HL-$BnCl_2$ (Chart 1), illustrating the easy exchange of the terminal ligand. Furthermore, we show that electrochemical oxidation of the $Fe^{III}Fe^{II}$ aqua complex to the diferric state induces the deprotonation of the aqua ligand. Mössbauer spectroscopy is sensitive to coordination changes in these kinds of complexes[19,20] and proved very helpful to characterize these ligand exchanges and transformations. The biological relevance of these reactions will be discussed.

Experimental Section

Materials. Acetonitrile (HPLC grade S) for electrochemistry was obtained from Rathburn Chemicals Ltd., stored under inert atmo-

(3) Stenkamp, R. E. *Chem. Rev.* **1994**, *94*, 715−726.
(4) Martins, L. J.; Hill, C. P.; Ellis, W. R. J. *Biochemistry* **1997**, *36*, 7044−7049.
(5) Farmer, C. S.; Kurtz, D. M. J.; Liu, Z. J.; Wang, B. C.; Rose, J.; Ai, J.; Sanders-Loehr, J. *JBIC* **2001**, *6*, 418−429.
(6) Scarrow, R. C.; Maroney, M. J.; Palmer, S. M.; Que, L. J.; Roe, A. L.; Salowe, S. P.; Stubbe, J. *J. Am. Chem. Soc.* **1987**, *109*, 7857−7864.
(7) Thomann, H.; Bernardo, M.; McCormick, J. M.; Pulver, S.; Andersson, K. K.; Lipscomb, J. D.; Solomon, E. I. *J. Am. Chem. Soc.* **1993**, *115*, 8881−8882.
(8) Pearce, L. L.; Kurtz, D. M. J.; Xia, Y. M.; Debrunner, P. G. *J. Am. Chem. Soc.* **1987**, *109*, 7286−7293.
(9) McCormick, J. M.; Solomon, E. I. *J. Am. Chem. Soc.* **1990**, *112*, 2005−2007.
(10) Wieghardt, K.; Pohl, K.; Gebert, W. *Angew. Chem., Int. Ed. Engl.* **1983**, *22*, 727−728.
(11) Armstrong, W.; Spool, A.; Papaefthymiou, G.; Frankel, R.; Lippard, S. *J. Am. Chem. Soc.* **1984**, *106*, 3653−3667.
(12) Mauerer, B.; Crane, J.; Schuler, J.; Wieghardt, K.; Nuber, B. *Angew. Chem., Int. Ed. Engl.* **1993**, *32*, 289−291.
(13) He, C.; Barrios, A. M.; Lee, D.; Kuzelka, J.; Davydov, R. D.; Lippard, S. J. *J. Am. Chem. Soc.* **2000**, *122*, 12683−12690.
(14) Mizoguchi, T. J.; Kuzelka, J.; Spingler, B.; DuBois, J. L.; Davydov, R. D.; Hedman, B.; Hodgson, K. O.; Lippard, S. J. *Inorg. Chem.* **2001**, *40*, 4662−4673.
(15) Kanda, W.; Moneta, W.; Bardet, M.; Bernard, E.; Debaecker, N.; Laugier, J.; Bousseksou, A.; Chardon-Noblat, S.; Latour, J. M. *Angew. Chem., Int. Ed. Engl.* **1995**, *34*, 588−590.
(16) Lambert, E.; Chabut, B.; Chardon-Noblat, S.; Deronzier, A.; Chottard, G.; Bousseksou, A.; Tuchagues, J. P.; Bardet, M.; Laugier, J.; Latour, J. M. *J. Am. Chem. Soc.* **1997**, *119*, 9424−9437.
(17) Satcher, J. H.; Balch, A. L.; Olmstead, M. M.; Droege, M. W. *Inorg. Chem.* **1996**, *35*, 1749−1750.
(18) Satcher, J. H.; Droege, M. W.; Olmstead, M. M.; Balch, A. L. *Inorg. Chem.* **2001**, *40*, 1454−1458.
(19) Borovik, A. S.; Papaefthymiou, V.; Taylor, L. F.; Anderson, O. P.; Que, L., Jr. *J. Am. Chem. Soc.* **1989**, *111*, 6183−6195.
(20) Maeda, Y.; Tanigawa, Y.; Hayami, S.; Takashima, Y. *Chem. Lett.* **1992**, 591−594.

sphere, and used without further purification. Acetonitrile for spectroscopic measurements was distilled over CaH_2 and stored within an inert-atmosphere glovebox. Dichloromethane was passed over alumina and stored under argon. All other reagents were of reagent grade quality and used as received. 1,3-Benzenedipropionic acid was prepared as described in the literature.[21]

Syntheses. The asymmetric binucleating phenol ligand HL-Bn and the corresponding diiron(II,III) complexes $[Fe^{III}$(L-Bn)(mpdp)-$Fe^{II}(H_2O)](BPh_4)_2$ or $[Fe^{III}$(L-Bn)(mpdp)$Fe^{II}(H_2O)](ClO_4)_2$ (Chart 1) were synthesized as described previously.[15] The 2,6-dichlorobenzyl ligand (HL-$BnCl_2$) and its diiron(II,III) complex were prepared similarly.[16] Anal. Calcd for $[Fe_2$(L-Bn)(mpdp)$(H_2O)](BPh_4)_2 \cdot 2H_2O$, $Fe_2C_{94}H_{92}N_5O_8B_2$: C, 72.69; H, 5.97; N, 4.51; Fe, 7.19. Found: C, 72.9; H, 5.9; N, 4.4; Fe, 6.9. Calcd for $[Fe_2$(L-$BnCl_2$)(mpdp)$(H_2O)](ClO_4)_2 \cdot 2H_2O$, $Fe_2C_{46}H_{50}N_5O_{16}Cl_4$: C, 46.73; H, 4.26; N, 5.92; Fe, 9.45. Found: C, 46.1; H, 4.3; N, 5.7; Fe, 9.5. FAB(+) mass spectrometry: $m/z = 1027$, $[Fe_2$ (L-$BnCl_2$)(mpdp)-$(ClO_4)]^+$.

Physicochemical Studies. Electronic absorption spectra were recorded on a Lambda 9 Perkin-Elmer spectrometer in acetonitrile. NMR spectra were recorded in deuterated acetonitrile on a Varian Unity 400 spectrometer with a 5 mm indirect detection operating at 400 MHz for the proton as described previously.[16]

Magnetic susceptibility experiments were done on a MPMS Quantum Design magnetometer operating at 0.5−5 T in the 2−300 K temperature range. The polycrystalline sample (ca. 15 mg) was contained in a kel F bucket which was calibrated independently. The susceptibility of the compound was corrected from the diamagnetism calculated using Pascal's constants.[22] The simulation of the data was conducted in two steps. First the data were fitted to the Van Vleck equation for two interacting spins $S = 2$ and $S = 5/2$ on the basis of the Heisenberg exchange Hamiltonian $H = -2JS_1S_2$.[22] Then a full treatment based on matrix diagonalization using the Hamiltonian

$$H = -2JS_1S_2 + \Sigma_i\{D_i[(S_{iz})^2 - (1/3)(S_i)(S_i + 1) + E_i[(S_{ix})^2 - (S_{iy})^2]\}$$

was used to obtain the zero-field splitting of the Fe^{2+} ion.[23] The R index $\{R = \Sigma[(\chi T_{exp}) - (\chi T_{cal})]^2/N\Sigma(\chi T_{exp})^2\}$ was 6.6×10^{-6}.

^{57}Fe Mössbauer experiments were performed using a 30 mCi source of ^{57}Co(Rh). The 14.4 keV γ-rays were detected by means of a proportional counter and Mössbauer spectra recorded on a 512 multichannel analyzer working in the multiscaling mode. The system was calibrated with a metallic iron absorber at room temperature, and all velocity scales and isomer shifts are referred to the iron standard. The temperature of the sample was measured with a Pt resistor. A conventional liquid-nitrogen, horizontal transmission cryostat was used; the source was maintained at room temperature and moved by a constant-acceleration electromechanical drive system under feedback control. The minimum observed line width (fwhm) was 0.25 mm/s.

Electrochemical measurements were done using an EG&G Princeton Applied Research model 173 potentiostat−galvanostat equipped with a Sefram TGM 164 X-Y recorder. All voltammograms were obtained in a conventional three-electrode cell under an argon atmosphere in a drybox (Jaram) with a dioxygen content lower than 5 ppm. Tetrabutylammonium perchlorate (TBAP) was used as supporting electrolyte. All potentials reported are relative to Ag|10 mM Ag^+ for acetonitrile solutions or Ag|AgCl (saturated LiCl in EtOH) for CH_2Cl_2 solutions and can be converted to the NHE by adding 0.548 or 0.22 V, respectively.[24] For cyclic voltammetry and exhaustive electrolyses the working electrode was a platinum disk (area = 0.2 cm^2) or plate (area = 5 cm^2), respectively. The spectroelectrochemical experiments were ran within a drybox in conventional cuvettes which were inserted into the optical translator connected through a fiber optic system (Photonics Spectrofip system) to a Hewlett-Packard 8452A diode array spectrophotometer.

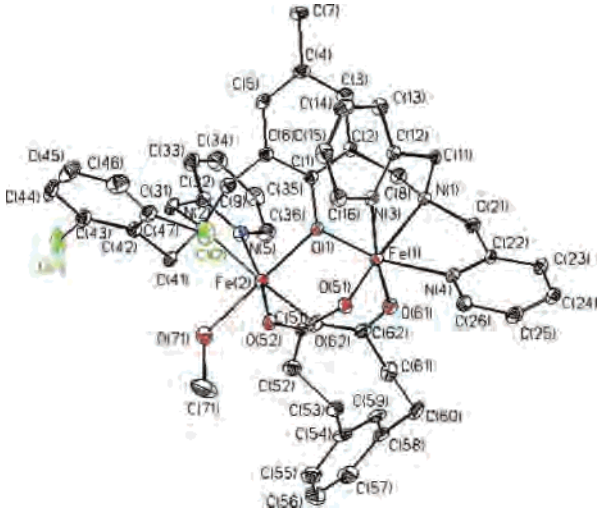

Figure 1. Structure of the cation $[Fe^{III}$(L-$BnCl_2$)(mpdp)$Fe^{II}(CH_3OH)]^{2+}$ with thermal ellipsoids at the 50% level.

Results

Part I: Syntheses and Solid-State Studies. Syntheses. $[Fe^{III}$(L-Bn)(mpdp)$Fe^{II}(H_2O)](BPh_4)_2$ was obtained by following a literature procedure[25] from the reaction in methanol of the ligand HL-Bn with 2 equiv of $Fe(NO_3)_3 \cdot 9H_2O$ and 1 equiv of disodium 1,3-benzenedipropionate followed by precipitation with $Na(BPh_4)$ and crystallization from an acetonitrile/methanol mixture.[15] Alternatively, the reaction can be performed under anaerobic conditions with $Fe(ClO_4)_2 \cdot 6H_2O$ and then exposed to air;[19] the desired complex $[Fe^{III}$(L-Bn)(mpdp)$Fe^{II}(H_2O)](ClO_4)_2$ crystallizes upon standing. Crystals of $[Fe^{III}$(L-$BnCl_2$)(mpdp)$Fe^{II}(CH_3OH)](ClO_4)_2$ suitable for an X-ray analysis have been obtained by slow evaporation of an acetonitrile/methanol mixture. The structures of the two compounds are very similar except for the replacement of the terminal aqua ligand on Fe^{II} by a methanol molecule (see below).

X-ray Structure of $[Fe^{III}$(L-$BnCl_2$)(mpdp)$Fe^{II}(CH_3OH)](ClO_4)_2$. Crystals of $[Fe^{III}$(L-$BnCl_2$)(mpdp)$Fe^{II}(CH_3OH)](ClO_4)_2$ consist of discrete cations $[Fe^{III}$(L-$BnCl_2$)(mpdp)-$Fe^{II}(CH_3OH)]^{2+}$ and perchlorate anions. The structure of the cation is illustrated in Figure 1. The crystal parameters are listed in Table 1, and important bond distances and angles are summarized in Table 2. The two iron ions are bridged

(21) Beer, R. H.; Tolman, W. B.; Bott, S. G.; Lippard, S. J. *Inorg. Chem.* **1989**, *28*, 4557−4559.
(22) Kahn, O. *Molecular Magnetism*; VCH: New York, 1993.
(23) Atta, M.; Scheer, C.; Fries, P. H.; Fontecave, M.; Latour, J. M. *Angew. Chem., Int. Ed. Engl.* **1992**, *31*, 1513−1515.
(24) Pavlishchuk, V. V.; Addison, A. W. *Inorg. Chim. Acta* **2000**, *298*, 97−102.
(25) Suzuki, M.; Uheara, A.; Oshio, H.; Endo, K.; Yanaga, M.; Kida, S.; Saito, K. *Bull. Chem. Soc. Jpn.* **1987**, *60*, 3547−3555.

Table 1. Crystal and Structure Refinement Data for $[Fe^{III}(L\text{-}BnCl_2)(mpdp)Fe^{II}(CH_3OH)](ClO_4)_2$

empirical formula	$C_{48}H_{52}Cl_4Fe_2N_5O_{15}$
fw	1192.45
temp	193(2) K
wavelength	0.710 73 Å
cryst system	monoclinic
space group	$P2_1/n$
unit cell dimens	$a = 13.3095(14)$ Å; $\alpha = 90°$
	$b = 20.1073(19)$ Å; $\beta = 94.471(2)°$
	$c = 19.4997(19)$ Å; $\gamma = 90°$
V, Z	5202.6(9) Å^3, 4
d(calcd)	1.522 Mg/m^3
abs coeff	0.835 mm^{-1}
F(000)	2460
cryst size	0.08 × 0.2 × 0.3 mm
θ range for data collcn	1.84−28.79°
limiting indices	$-17 \le h \le 11$, $-21 \le k \le 21$, $-18 \le l \le 26$
reflcns collcd	12 993
indpndt reflcs	9004 [R(int) = 0.0348]
abs corr	none
refinement method	full-matrix least-squares on F^2
data/restraints/params	9004/0/875
goodness-of-fit on F^2	1.072
final R indices [$I > 2\sigma(I)$]	R1 = 0.0666, wR2 = 0.1521
R indices (all data)	R1 = 0.1135, wR2 = 0.2013
largest diff peak and hole	1.416 and −1.144 e·Å^{-3}

Table 2. Important Bond Lengths and Angles for $[Fe^{III}(L\text{-}BnCl_2)(mpdp)Fe^{II}(CH_3OH)](ClO_4)_2$

Fe(1)−O(51)	1.9429(18)	Fe(2)−O(62)	2.070(2)
Fe(1)−O(1)	1.9490(15)	Fe(2)−O(1)	2.0928(16)
Fe(1)−O(61)	1.9630(18)	Fe(2)−O(52)	2.1055(18)
Fe(1)−N(4)	2.1426(19)	Fe(2)−O(71)	2.1180(19)
Fe(1)−N(3)	2.171(2)	Fe(2)−N(5)	2.143(2)
Fe(1)−N(1)	2.200(2)	Fe(2)−N(2)	2.276(2)
O(51)−Fe(1)−O(1)	101.38(7)	O(62)−Fe(2)−O(1)	90.44(7)
O(51)−Fe(1)−O(61)	99.30(8)	O(62)−Fe(2)−O(52)	94.12(7)
O(1)−Fe(1)−O(61)	93.25(7)	O(1)−Fe(2)−O(52)	90.22(7)
O(51)−Fe(1)−N(4)	93.53(8)	O(62)−Fe(2)−O(71)	90.36(8)
O(1)−Fe(1)−N(4)	164.88(8)	O(1)−Fe(2)−O(71)	176.76(7)
O(61)−Fe(1)−N(4)	86.75(8)	O(52)−Fe(2)−O(71)	86.59(7)
O(51)−Fe(1)−N(3)	89.61(8)	O(62)−Fe(2)−N(5)	95.40(8)
O(1)−Fe(1)−N(3)	87.99(7)	O(1)−Fe(2)−N(5)	91.64(7)
O(61)−Fe(1)−N(3)	170.55(8)	O(52)−Fe(2)−N(5)	170.29(8)
N(4)−Fe(1)−N(3)	89.61(7)	O(71)−Fe(2)−N(5)	91.41(8)
O(51)−Fe(1)−N(1)	163.61(7)	O(62)−Fe(2)−N(2)	172.96(8)
O(1)−Fe(1)−N(1)	89.27(7)	O(1)−Fe(2)−N(2)	87.45(7)
O(61)−Fe(1)−N(1)	92.41(8)	O(52)−Fe(2)−N(2)	92.61(7)
N(4)−Fe(1)−N(1)	75.63(7)	O(71)−Fe(2)−N(2)	92.11(7)
N(3)−Fe(1)−N(1)	78.23(8)	N(5)−Fe(2)−N(2)	77.96(8)

by the phenolate oxygen O1 and the two carboxylate groups of the mpdp ligand. The coordination of Fe1 is complemented by the three nitrogen atoms of the bis(picolyl)amine branch. The overall N_3O_3 coordination around Fe1 corresponds to a rhombically distorted octahedron. The coordination of Fe2 is complemented by the two nitrogen atoms N2 and N5 from the tertiary amine and the pyridine group, respectively, and by O71 from the methanol molecule. Examination of the bond distances in Table 2 shows that they average 2.061 Å around Fe1 and 2.134 Å around Fe2. The latter is close to that found in diferrous bis(μ-propionato)[26] and bis(μ-diphenylphosphato)[27] complexes of the tetrapyridyl ligand: 2.151 and 2.138 Å, respectively. In the analogous bis(μ-propionato) complex in the mixed-valent $Fe^{II}Fe^{III}$ state, the average Fe−ligand distance to the ferric site is shorter than that to the ferrous one (2.056 vs 2.131 Å), as expected. From this 0.075 Å difference it was concluded that the valences of the two ions are localized. A similar difference 0.073 Å is observed for **1,** which indicates that the valences of the two iron atoms are localized and that Fe1 is the Fe^{3+} site and Fe2 the Fe^{2+} one. The distance Fe2−O71 between the Fe^{2+} ion and the methanol oxygen is 2.118 Å, which is very similar to the distance (2.156 Å) between the Fe^{2+} ion and the oxygen of the aqua ligand in $[Fe^{III}(L\text{-}Bn)(mpdp)Fe^{II}(H_2O)](BPh_4)_2$.[15]

Magnetic Susceptibility. The magnetic properties of $[Fe^{III}(L\text{-}Bn)(mpdp)Fe^{II}(H_2O)](BPh_4)_2$ were investigated over the range 2−300 K at six magnetic fields between 0.5 and 5 T. The product of the molar susceptibility by temperature decreases smoothly from ca. 7 cm^3·K·mol^{-1} at 300 K to ca. 5.7 cm^3·K·mol^{-1} at 100 K and then more abruptly to reach 0.4 cm^3·K·mol^{-1} at 2 K (Figure S1, Supporting Information). Such a behavior is characteristic of antiferromagnetically coupled systems. This temperature dependence of χT could be simulated at 0.5 T by using the Van Vleck equation derived from the Heisenberg exchange Hamiltonian for two interacting spins $S_1 = 2$ and $S_2 = 5/2$. The best fit was obtained for an exchange interaction $J = -3.2$ cm^{-1}. Nevertheless, below 30 K the simulation was of poorer quality. This was due to the fact that the anisotropy of the system was neglected in the calculation. Indeed, owing to spin−orbit coupling, Fe^{2+} ions can have substantial axial zero-field splittings, up to 20 cm^{-1},[28] such that the condition $D \ll J$ is not fulfilled and Van Vleck's equation is not valid. Therefore, a matrix diagonalization procedure was used.[23] To avoid an overparametrization of the system, it was assumed that the Fe^{3+} ion has an isotropic **g** tensor and no zero-field splitting ($g_3 = 2.0$, $D_3 = E_3 = 0$) and that the zero-field splitting tensor of the Fe^{2+} ion was not rhombic ($E_2 = 0$). The best fit parameters thus obtained are $J = -3.2(2)$ cm^{-1}, $g_2 = 2.07(3)$, and $D_2 = 9.2(8)$ cm^{-1}.

Part II: Acetonitrile/Aqua Ligand Exchange. The present and past X-ray characterization of these mixed-valent complexes shows that a ligand exchange on the Fe^{2+} site can be easily achieved. Since this process is likely to modify the electronic properties of the diiron center, we decided to investigate the aqua/acetonitrile exchange through spectroscopic and electrochemical methods.

Electronic Absorption Spectroscopy. The electronic absorption spectra of mixed-valent $Fe^{II}Fe^{III}$ complexes of μ-phenolato ligands are dominated in the visible region by an intense band ($\epsilon = 900-1000$ mol^{-1}·L·cm^{-1}) close to 550 nm which is assigned to the charge transfer from the bridging phenolate ligand to the Fe^{3+} ion (LMCT p$\pi \rightarrow$ dπ^*).[19,25] When the complexes $[Fe^{III}(L\text{-}Bn)(mpdp)Fe^{II}(H_2O)](BPh_4)_2$ or $[Fe^{III}(L\text{-}BnCl_2)(mpdp)Fe^{II}(CH_3OH)](ClO_4)_2$ are dissolved in acetonitrile, their solutions exhibit the same absorption band at 578 nm (17 300 cm^{-1}, $\epsilon = 1300$ mol^{-1}·L·cm^{-1})

(26) Borovik, A. S.; Hendrich, M. P.; Holman, T. R.; Münck, E.; Papaefthymiou, V.; Que, L., Jr. *J. Am. Chem. Soc.* **1990**, *112*, 6031−6038.

(27) Jang, H.; Hendrich, M.; Que, L., Jr. *Inorg. Chem.* **1993**, *32*, 911−918.

(28) Solomon, E.; Pavel, E.; Loeb, K.; Campochiaro, C. *Coord. Chem. Rev.* **1995**, *144*, 369−460.

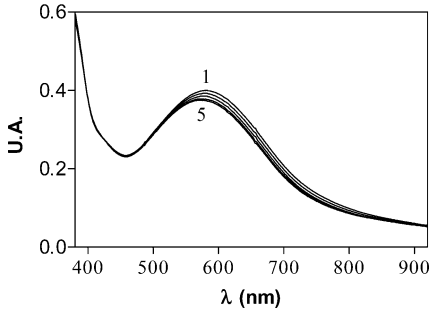

Figure 2. Electronic absorption spectrum of $[Fe^{III}(L\text{-}Bn)(mpdp)Fe^{II}(CH_3CN)]^{2+}$ in acetonitrile (1) with successive additions of water: 400, 800, 1200, and 1600 molar equiv (5).

(Figure 2, curve 1). This indicates that, upon dissolution in acetonitrile, the exogeneous aqua/methanol ligand is substituted by an acetonitrile molecule leading to the formation of $[Fe^{III}(L\text{-}Bn)(mpdp)Fe^{II}(CH_3CN)]^{2+}$. Progressive addition of water causes this band to move from 578 to 569 nm (17 575 cm^{-1}, $\epsilon = 1050\ mol^{-1}\cdot L\cdot cm^{-1}$) with a slight loss of intensity (Figure 2). This transformation is quantitative after addition of ca. 1500 molar equiv of water (Figure 2, curve 5) and occurs with an isosbestic point at 947 nm (Figure S2). These observations are consistent with an initial replacement of the exogeneous ligand present in the solid state (H_2O or CH_3OH) by acetonitrile and then a simple transformation of the acetonitrile complex cation $[Fe^{III}(L\text{-}Bn)(mpdp)Fe^{II}(CH_3CN)]^{2+}$ into the aqua one $[Fe^{III}(L\text{-}Bn)(mpdp)Fe^{II}(H_2O)]^{2+}$ (eq 1).

$$[Fe^{III}(L\text{-}Bn)(mpdp)Fe^{II}(CH_3CN)]^{2+} \underset{CH_3CN}{\overset{H_2O}{\rightleftharpoons}} [Fe^{III}(L\text{-}Bn)(mpdp)Fe^{II}(H_2O)]^{2+} \quad (1)$$

The study of the temperature dependence of the equilibrium showed that formation of the acetonitrile complex is favored at low temperature. Nevertheless, owing to the small spectroscopic changes (see Figure 2), it was impossible to quantitate precisely this effect.

NMR Spectroscopy. The NMR spectrum of $[Fe^{III}(L\text{-}Bn)(mpdp)Fe^{II}(CH_3CN)]^{2+}$ in acetonitrile extends over more than 600 ppm, from 555 to −48 ppm (Figure 3a). Such a behavior departs drastically from that of the mixed-valent complexes of the tetrapyridyl[19] (Hbpmp) and tetraimidazolyl[29] ligands whose spectral range covers only 400 ppm and is restricted to positive chemical shifts. The wide spectral range of $[Fe^{III}(L\text{-}Bn)(mpdp)Fe^{II}(CH_3CN)]^{2+}$ results from a combination of (i) the very weak magnetic exchange interaction between the high-spin Fe^{2+} ($S = 2$) and Fe^{3+} ($S = 5/2$) ions and (ii) the fact that their valences are localized on the NMR time scale.[15] Assignments of the signals were made by chemical substitution (replacement of mpdp by acetate), T_1 measurements, and COSY experiments as well as by comparisons with related compounds.[19,30,31]

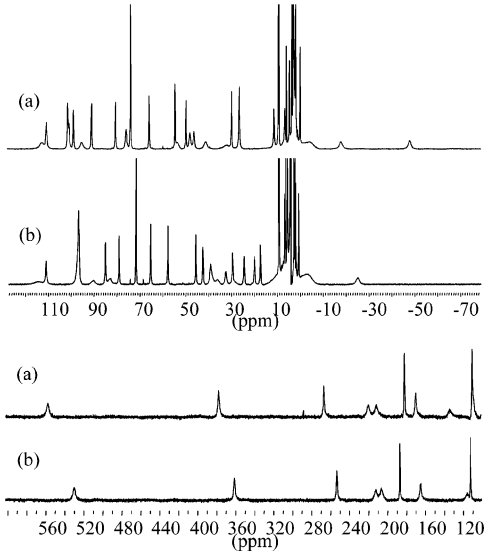

Figure 3. NMR spectrum of $[Fe^{III}(L\text{-}Bn)(mpdp)Fe^{II}(CH_3CN)]^{2+}$ in acetonitrile in the absence (a) and in the presence (b) of 1500 molar equiv of D_2O.

The spectrum of $[Fe^{III}(L\text{-}Bn)(mpdp)Fe^{II}(CH_3CN)]^{2+}$ (Figure 3a) bears a strong resemblance with those of the $[Fe^{II}Fe^{III}]$ complexes of the asymmetrical ligands (HL-BnOH and HL-PhOH) providing a terminal phenolate to one iron ion.[16] This allows one to assign quite confidently the three extreme downfield resonances at 555, 375, and 265 ppm to the equatorial methylenic protons[32] of the branch bound to the Fe^{3+} ion.[30] The three very wide resonances at 219, 210, and 137 ppm correspond to the *ortho*-pyridyl protons: their short distances to the metal ions is responsible for their short T_2. The observation of two resonances more downfield shifted than the third one indicates that the Fe^{3+} ion with the larger spin is bound in the branch possessing two pyridines, thereby confirming the valence localization found in the solid state. The peculiar upfield shifted resonance at −48 ppm is assigned to the equatorial methylenic proton of the third picolyl group bound to the Fe^{2+} ion. $[Fe^{III}(L\text{-}BnCl_2)(mpdp)Fe^{II}(CH_3CN)]^{2+}$ possesses a closely similar spectrum except for the lack of a peak at 95 ppm which we assign therefore to the *ortho*-benzylic protons of $[Fe^{III}(L\text{-}Bn)(mpdp)Fe^{II}(CH_3CN)]^{2+}$.

Progressive addition of D_2O causes important shifts (10−30 ppm) of several signals which stabilize after addition of ca. 1500 molar equiv of D_2O (Figure 3b). The signals experiencing the most important shifts are those associated with the *ortho*-pyridinyl and methylenic protons which are closer to the iron atoms. It is especially noteworthy that while most signals exhibit upfield shifts, two of them located at 74 and −48 ppm in $[Fe^{III}(L\text{-}Bn)(mpdp)Fe^{II}(CH_3CN)]^{2+}$ and 78 and −45 ppm in $[Fe^{III}(L\text{-}BnCl_2)(mpdp)Fe^{II}(CH_3CN)]^{2+}$ exhibit downfield shifts of more than 20 ppm. These signals are assigned, respectively, to the axial and equatorial methylenic protons of the picolyl group bound to the Fe^{2+} ion. Their peculiar behavior may therefore result from the anisotropy of the Fe^{2+} ion. As a consequence of these shifts,

(29) Mashuta, M.; Webb, R. J.; McCluster, J. K.; Schmitt, E. A.; Oberhausen, K. J.; Richardson, J. F.; Buchanan, R. M.; Hendrickson, D. N. *J. Am. Chem. Soc.* **1992**, *114*, 4−115, 3815−3827.
(30) Ming, L. J.; Jang, H. G.; Que, L., Jr. *Inorg. Chem.* **1992**, *31*, 359−364.
(31) Wang, Z.; Holman, T. R.; Que, L., Jr. *Magn. Reson. Chem.* **1993**, *31*, S78−S83.

(32) Axial and equatorial methylenic protons are defined by analogy with cyclohexane.

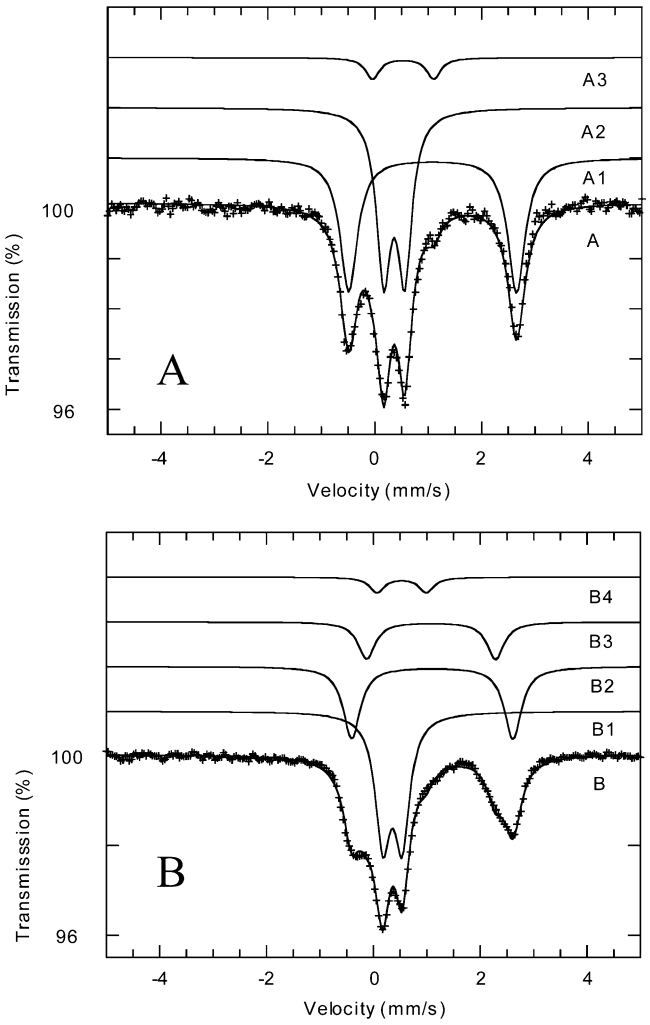

Figure 4. Mössbauer spectra at 77 K of acetonitrile solution of $[Fe^{III}(L\text{-}Bn)(mpdp)Fe^{II}(CH_3CN)]^{2+}$ in the absence (A) and in the presence (B) of 1500 equiv of water.

a significant decrease of the spectrum range to ca. 550 ppm is observed.

Mössbauer Spectroscopy. The zero-field Mössbauer spectrum of $[Fe^{III}(L\text{-}Bn)(mpdp)Fe^{II}(CH_3CN)]^{2+}$ in acetonitrile solution at 77 K is shown in Figure 4A together with its deconvolution into individual iron sites (solid lines above the experimental spectrum).

It consists of two quadrupole doublets (traces A1 and A2) of equal relative areas with isomer shifts δ/Fe = 1.20(1) and 0.48(1) mm/s and quadrupole splittings ΔE_Q = 3.14(1) and 0.39(1) mm/s. A high-spin Fe^{3+} impurity (trace A3, δ/Fe = 0.64(2) mm/s, ΔE_Q = 1.0(1) mm/s) is also present (6(1)%). The first doublet (trace A1) is attributed to the high-spin Fe^{2+} center, while the second one (trace A2) corresponds to the high-spin Fe^{3+} center of the mixed-valent complex.

Figure 4B shows the zero-field Mössbauer spectrum obtained after addition of 1500 equiv of water to an acetonitrile solution of $[Fe^{III}(L\text{-}Bn)(mpdp)Fe^{II}(CH_3CN)]^{2+}$. At first we note the presence of a high-spin Fe^{3+} impurity (trace B4, 6%) as found in the $[Fe^{III}(L\text{-}Bn)(mpdp)Fe^{II}(CH_3CN)]^{2+}$ sample (see trace A3 of Figure 4A). Apart from this impurity, the spectrum can be fitted by considering three distinct iron sites. The first site (trace B1, 47(1)%) corresponds to an Fe^{3+} center with Mössbauer parameters δ/Fe = 0.47(1) mm/s and ΔE_Q = 0.36(1) mm/s. These parameters are similar to those obtained for the Fe^{3+} center in $[Fe^{III}(L\text{-}Bn)(mpdp)Fe^{II}(CH_3CN)]^{2+}$ (see trace A2 of Figure 4A) and in $[Fe^{III}(L\text{-}Bn)(mpdp)Fe^{II}(H_2O)](BPh_4)_2$ (δ/Fe = 0.475(4) mm/s and ΔE_Q = 0.329(6) mm/s).[16] The second and third sites (trace B2, 31(1)%, and trace B3, 16(1)%, respectively) correspond to two Fe^{2+} centers with similar isomer shift values δ/Fe = 1.21(1) and 1.19(1) mm/s but different quadrupole splitting values ΔE_Q = 3.02(2) and 2.41(2) mm/s, respectively. The parameters associated with the second site are close to those obtained for the Fe^{2+} center in $[Fe^{III}(L\text{-}Bn)(mpdp)Fe^{II}(CH_3CN)]^{2+}$ (see trace A1 of Figure 4A) while those obtained for the third site are close to those published for the $Fe^{II}N_2O_3(OH_2)$ site in $[Fe^{III}(L\text{-}Bn)(mpdp)Fe^{II}(H_2O)](BPh_4)_2$ (δ/Fe = 1.196(4) mm/s and ΔE_Q = 2.657(7) mm/s).[15] The latter observation suggests that the three iron sites are associated with two dinuclear species. Indeed, the second iron site (trace B2) corresponds to the Fe^{2+} center in the remaining starting $[Fe^{III}(L\text{-}Bn)(mpdp)Fe^{II}(CH_3CN)]^{2+}$ complex, whereas the third iron site (trace B3) is associated with the $Fe^{2+}-OH_2$ center in $[Fe^{III}(L\text{-}Bn)(mpdp)Fe^{II}(H_2O)]^{2+}$. Under this assumption, the first iron site (trace B1) corresponds to the Fe^{3+} center in the starting $[Fe^{III}(L\text{-}Bn)(mpdp)Fe^{II}(CH_3CN)]^{2+}$ complex (≈62%) as well as the Fe^{3+} center in a new complex (namely $[Fe^{III}(L\text{-}Bn)(mpdp)Fe^{II}(H_2O)]^{2+}$, ≈32%) generated from $[Fe^{III}(L\text{-}Bn)(mpdp)Fe^{II}(CH_3CN)]^{2+}$ by water substitution of the CH_3CN ligand. We did not notice any improvement in the fitting procedure by considering four iron sites, i.e. by considering slightly different Mössbauer parameters for each of the Fe^{3+} centers in $[Fe^{III}(L\text{-}Bn)(mpdp)Fe^{II}(CH_3CN)]^{2+}$ and $[Fe^{III}(L\text{-}Bn)(mpdp)Fe^{II}(H_2O)]^{2+}$ complexes. The Mössbauer parameters obtained for all iron sites in $[Fe^{III}(L\text{-}Bn)(mpdp)Fe^{II}(CH_3CN)]^{2+}$ and $[Fe^{III}(L\text{-}Bn)(mpdp)Fe^{II}(H_2O)]^{2+}$ are summarized in Table 3.

In conclusion, it appears that the values of the isomer shifts of the Fe^{2+} sites for the aqua and acetonitrile complexes are quite similar whereas the values of their quadrupole splittings are significantly different. Indeed, acetonitrile substitution of the terminal water results in a significant increase of the quadrupole splitting value of the Fe^{2+} site (+0.5 mm/s).

Electrochemical Study. To further characterize the terminal exchange reaction, the electrochemical properties of $[Fe^{III}(L\text{-}Bn)(mpdp)Fe^{II}(CH_3CN)]^{2+}$ and $[Fe^{III}(L\text{-}Bn)(mpdp)Fe^{II}(H_2O)]^{2+}$ have been investigated in acetonitrile and methylene chloride solutions, respectively. Cyclic voltammograms of a solution of $[Fe^{III}(L\text{-}Bn)(mpdp)Fe^{II}(CH_3CN)]^{2+}$ at a platinum disk in CH_3CN are depicted in Figure 5. In the anodic region (Figure 5, curve a) a reversible couple is observed at $E_{1/2}$(ox) = 0.53 V vs Ag|10 mM Ag^+ (E_{pa} = 0.57 V, E_{pc} = 0.49 V, ΔE_p = 0.08 V) corresponding to the reversible one-electron oxidation of the Fe^{2+} center of the mixed-valent $Fe^{II}Fe^{III}$ complex (eq 2).

$$[Fe^{III}(L\text{-}Bn)(mpdp)Fe^{II}(CH_3CN)]^{2+} \rightleftarrows [Fe^{III}(L\text{-}Bn)(mpdp)Fe^{III}(CH_3CN)]^{3+} + e^- \quad (2)$$

Table 3. Mössbauer Data for Mixed-valent and Diferric Complexes[a]

compd	site 1 ($Fe^{III}N_3O_3$)			site 2		
	δ/Fe	ΔE_Q	G	δ/Fe	ΔE_Q	G
Mixed-Valent Complexes						
$[Fe_2(L\text{-}Bn)(mpdp)(CH_3CN)]^{2+}$	0.48(1)	0.39(1)	0.39(1)	1.20(1)	3.14(1)	0.39(1)
$[Fe_2(L\text{-}Bn)(mpdp)(H_2O)]^{2+}$	0.47(1)	0.36(1)	0.38(1)	1.19(1)	2.41(2)	0.38(1)
$[Fe_2(L\text{-}Bn)(mpdp)(H_2O)](BPh_4)_2$[15]	0.475(4)	0.329(6)	0.198(6)	1.196(4)	2.657(7)	0.217(7)
$[Fe_2(bpmp)(OAc)_2(BF_4)_2$[19]	0.47	0.51	0.33	1.16	2.42	0.41
$[Fe_2(L\text{-}BnO)(dpp)_2](PF_6)$[16]	1.183(4)	3.358(7)	0.296(8)	0.550(5)	1.220(7)	0.296(8)
Diferric Complexes						
$[Fe_2(L\text{-}Bn)(mpdp)(CH_3CN)]^{3+}$	0.47(1)	0.40(1)	0.48(1)	0.40(1)	0.25(1)	0.48(1)
$[Fe_2(L\text{-}Bn)(mpdp)(H_2O)]^{3+}$	0.48(1)	0.44(1)	0.41(1)	0.55(1)	0.60(1)	0.41(1)
$[Fe_2(L\text{-}Bn)(mpdp)(OH)]^{2+}$	0.48(1)	0.44(1)	0.41(1)	0.55(1)	1.51(1)	0.41(1)
$[Fe_2(L\text{-}BnO)(dpp)_2](PF_6)_2$[16]	0.447(5)	0.31(2)	0.53(2)	0.57(2)	0.99(2)	0.53(2)

[a] δ/F_e = isomer shift (mm/s) with respect to metallic iron at room temperature. ΔE_Q = quadrupole splitting (mm/s). Γ = width at half-maximum of the Lorentzian lines (mm/s). Standard deviations are given in parentheses, in units of the last digit of quoted value.

Exhaustive electrolysis of the solution at 0.80 V requires 1 mol of electrons/mol of $[Fe^{III}(L\text{-}Bn)(mpdp)Fe^{II}(CH_3CN)]^{2+}$ and generates quantitatively the diiron(III,III) complex as judged from analysis of the resulting voltammogram. An exhaustive electrolysis at 0.35 V of this oxidized solution regenerates the starting complex showing the total reversibility of the system.

In the cathodic domain (Figure 5, curve b), the cyclic voltammogram exhibits a reversible one-electron reduction of the Fe^{3+} center of the mixed-valent complex (eq 3) with $E_{1/2}(red) = -0.35$ V ($E_{pa} = -0.31$ V; $E_{pc} = -0.39$ V, $\Delta E_p = 0.08$ V).

The exhaustive reduction at -0.70 V leads quantitatively to the diferrous complex ($\lambda_{max} = 420$ nm).[26] The complete regeneration of $[Fe^{III}(L\text{-}Bn)(mpdp)Fe^{II}(CH_3CN)]^{2+}$ by reoxidation at 0 V proves the reversibility of the one-electron-transfer process.

$$[Fe^{III}(L\text{-}Bn)(mpdp)Fe^{II}(CH_3CN)]^{2+} + e^- \rightleftarrows [Fe^{II}(L\text{-}Bn)(mpdp)Fe^{II}(CH_3CN)]^{+} \quad (3)$$

In methylene chloride, a solution of $[Fe^{III}(L\text{-}Bn)(mpdp)Fe^{II}(H_2O)]^{2+}$ exhibits the same electrochemical pattern with two reversible redox processes, but significant shifts are observed in half-wave potentials at $E_{1/2}(ox) = 0.80$ V and $E_{1/2}(red) = 0.13$ V vs Ag/saturated AgCl/LiCl (which corresponds to $E_{1/2}(ox) = 0.48$ V and $E_{1/2}(red) = -0.19$ V vs Ag/10 mM Ag^+).[24]

The ligand exchange (CH_3CN/H_2O) reaction can be also studied by electrochemistry. Progressive addition of water in a CH_3CN + 0.1 M TBAP solution containing $[Fe^{III}(L\text{-}Bn)(mpdp)Fe^{II}(CH_3CN)]^{2+}$ causes a decrease of the potential ($E_{1/2}(ox)$) of the $Fe^{III}Fe^{II}/Fe^{III}Fe^{III}$ couple (Figure 5, curve c, at 1500 molar equiv of H_2O) to a maximum of $\Delta E_{1/2}(ox) = -0.21$ V. At the same time, the variation ($\Delta E_{1/2}(red)$) of the potential of the $Fe^{II}Fe^{II}/Fe^{III}Fe^{II}$ couple is small (-0.03 V), which is consistent with the coordination of the N_3O_3 site being mostly unchanged (Figure 5, curve d).

The reverse exchange (H_2O/CH_3CN) was studied by progressive addition of CH_3CN in CH_2Cl_2 + 0.1 M TBAP electrolyte containing $[Fe^{III}(L\text{-}Bn)(mpdp)Fe^{II}(H_2O)]^{2+}$. As expected, the potential of the anodic peak of the $Fe^{III}Fe^{II}/Fe^{III}Fe^{III}$ system increases with the concentration of CH_3CN.

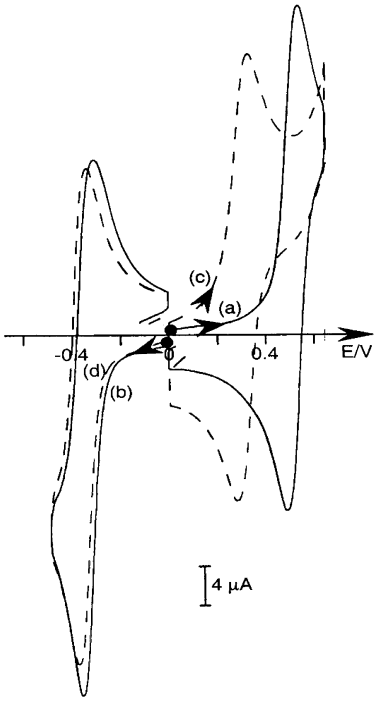

Figure 5. Cyclic voltammograms of $[Fe^{III}(L\text{-}Bn)(mpdp)Fe^{II}(CH_3CN)]^{2+}$ in acetonitrile in the absence (a, b) and in the presence (c, d) of 1500 molar equiv of water.

Scheme 1

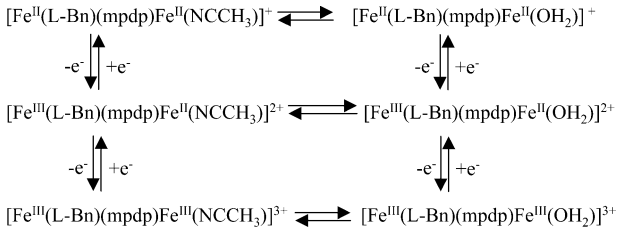

It reaches a stable value of 0.95 V after addition of 7200 molar equiv. However, the redox process is more complicated than a simple acetonitrile/water exchange. Actually, on the reverse scan the potential of the corresponding cathodic peak decreases indicating that the process becomes less reversible (see below). This observation suggests that a chemical reaction is occurring at this stage. Scheme 1 summarizes the transformations of the mixed-valent complex occurring during the exogen ligand exchanges and the redox processes.

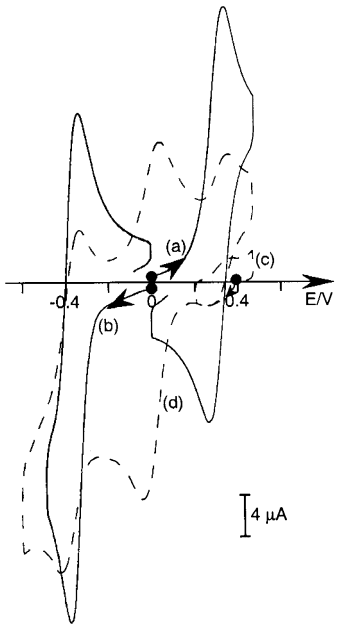

Figure 6. Cyclic voltammograms of $[Fe^{III}(L\text{-}Bn)(mpdp)Fe^{II}(CH_3CN)]^{3+}$ in acetonitrile + 7% water before (a, b) and after (c, d) electrolysis.

Part III: Oxidatively-Induced Deprotonation. Electrochemical Study. As detailed below, by studying the oxidation reaction of the mixed-valent aqua complex $[Fe^{III}(L\text{-}Bn)(mpdp)Fe^{II}(H_2O)]^{2+}$, we have shown that the diferric aqua complex is not stable on the time scale of an exhaustive electrolysis. A bulk electrolysis conducted at 0.50 V of an hydroorganic solution (7% H_2O in CH_3CN + 0.1 M TBAP) of $[Fe^{III}(L\text{-}Bn)(mpdp)Fe^{II}(H_2O)]^{2+}$ requires 1 electron/molecule. The electrochemical response of the resulting solution presents a new intense reversible system at $E_{1/2}(ox) = 0.00$ V ($E_{pa} = 0.04$ V; $E_{pc} = -0.04$ V; $\Delta E_p = 0.08$ V (Figure 6, curves c and d) besides the redox systems at $E_{1/2}(ox) = 0.33$ V and $E_{1/2}(red) = -0.39$ V of the remaining aqua complex (Figure 6, curves a and b, or Figure 5, curves c and d). Moreover, the formation of these two diferric complexes is clearly demonstrated by voltamperometry experiments using a Pt rotating disk electrode. Comparison of the wave heights of voltamperograms shows that the ratio of the two species in the mixture is ca. 90:10 in favor of the new species.

The new species exhibits a reduction potential less positive than the aqua and acetonitrile diferric complexes. The resulting solution has an absorption band located at 598 nm, while that of the acetonitrile diferric complex is at 604 nm, as seen previously. These observations are consistent with the presence of a bis Fe^{III} complex having an increase of the electron density on the two metal ions. Indeed, $E_{1/2}(ox)$ values of the mixed-valent complexes with a terminal phenolate in place of the terminal water ligand are also located around 0 V.[16] The similarity of the new species with the latter complexes is clearly evidenced by Mössbauer spectroscopy which shows that the external Fe^{3+} ion is bound by an anionic ligand (see next section). Electrochemical behavior and spectroscopic properties are thus in agreement with the existence of a diferric hydroxo complex in chemical equilibrium with the diferric aqua complex (eq 4).

Scheme 2

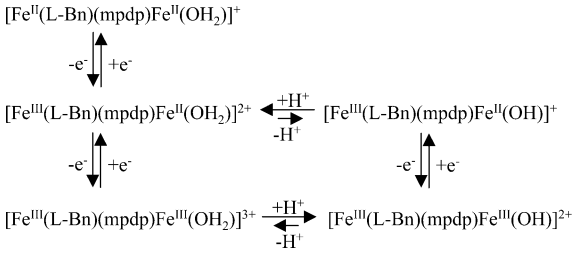

The formation of the hydroxo complex is a chemically reversible process since the reduction at −0.10 V of the oxidized solution regenerates quantitatively the starting aqua complex after consumption of 1 Faraday/mol.

$$[Fe^{III}(L\text{-}Bn)(mpdp)Fe^{III}(H_2O)]^{3+} \rightleftarrows [Fe^{III}(L\text{-}Bn)(mpdp)Fe^{III}(OH)]^{2+} + H^+ \quad (4)$$

It appears from the cyclic voltammograms (Figure 6, curves c and d) that the electrogenerated mixed-valence species $Fe^{III}Fe^{II}(OH^-)$ is unstable on the cyclic voltammetry time scale. On the reverse scan the intensity of the anodic peak of the $Fe^{III}Fe^{II}(H_2O)/Fe^{III}Fe^{III}(H_2O)$ couple is markedly larger than that of the aqua diferric complex remaining after exhaustive oxidation of $[Fe^{III}(L\text{-}Bn)(mpdp)Fe^{II}(H_2O)]^{2+}$. This indicates that the mixed-valent hydroxo species $[Fe^{III}(L\text{-}Bn)(mpdp)Fe^{II}(OH)]^+$ is rapidly protonated (Scheme 2). This observation is supported by the fact that the ratio of the respective anodic peak intensities of the $Fe^{III}Fe^{II}(H_2O)/Fe^{III}Fe^{III}(H_2O)$ and $Fe^{III}Fe^{II}(OH)/Fe^{III}Fe^{III}(OH)$ couples increases when the scanning rate decreases (from 500 to 20 $mV \cdot s^{-1}$). It must be noted also that in the reduction domain only the $Fe^{II}Fe^{II}(H_2O)/Fe^{III}Fe^{II}(H_2O)$ couple is observed, which suggests that the reduction of $Fe^{III}Fe^{II}(OH)$ is slower than the protonation rate of either $[Fe^{III}(L\text{-}Bn)(mpdp)Fe^{II}(OH)]^+$ or its reduced species $Fe^{II}Fe^{II}(OH)$.

The diferric hydroxo complex can be directly obtained through an oxygen ligand exchange at the $Fe^{III}Fe^{III}$ redox level by adding water to an electrogenerated $Fe^{III}Fe^{III}$ acetonitrile complex in CH_3CN solution. Obviously, the proportion of the equilibrium between the $Fe^{III}Fe^{III}(H_2O)$ and $Fe^{III}Fe^{III}(OH)$ species depends on the quantity of added water. The amount of the latter complex increases with the water content and reaches a maximum close to 70% for 8000 molar equiv of water added (data not shown). As shown in eq 4, the formation of the hydroxo diferric complex was accompanied by a release of protons. The presence of these protons in electrolyte solution is easily detected on the cyclic voltammogram by an increase of the irreversibility of the $[Fe^{III}(L)Fe^{II}(OH_2)]^{2+}/[Fe^{II}(L)Fe^{II}(OH_2)]^+$ redox system at $E_{1/2} = -0.39$ V. Indeed, addition of $HClO_4$ (2 molar equiv) to a solution of the $Fe^{III}Fe^{III}$ complex affects the voltammogram in the manner just described above (data not shown). This result confirms the existence of a dynamic equilibrium between the aqua and hydroxo complexes. Scheme 2 summarizes the different redox and chemical coupled reactions between the characterized species present after an exhaustive oxidation of the aqua mixed-valent complex.

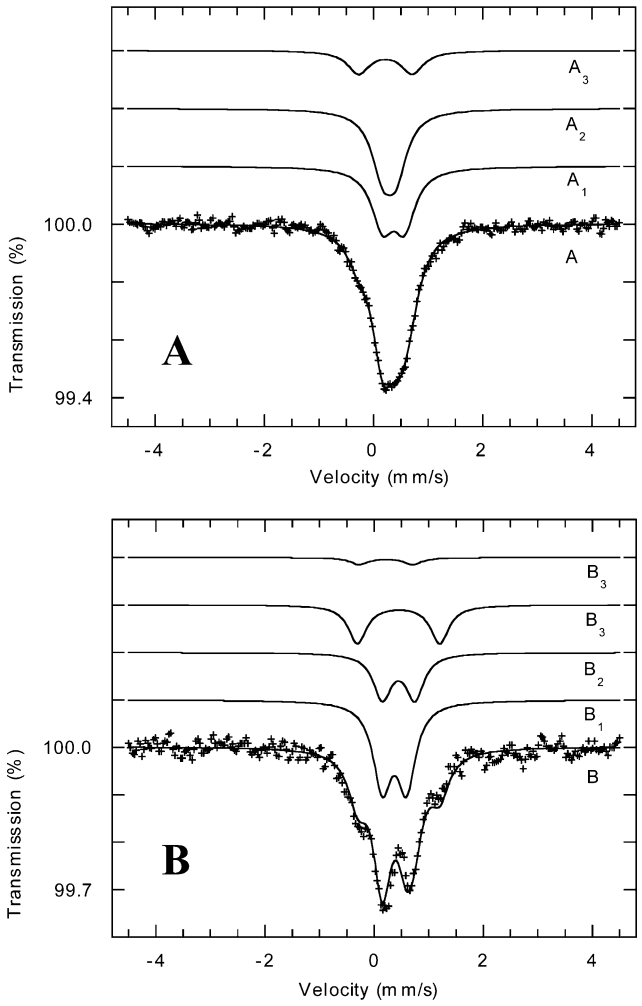

Figure 7. Mössbauer spectra at 77 K of an acetonitrile solution of $[Fe^{III}(L\text{-}Bn)(mpdp)Fe^{III}(CH_3CN)]^{3+}$ before (A) and after (B) addition of 1500 equiv of water.

Attempts to prepare the mixed-valent hydroxo complex by chemical deprotonation with an organic base or by adding OH^- ion to $[Fe^{III}(L\text{-}Bn)(mpdp)Fe^{II}(H_2O)]^{2+}$ have failed so far to give the hydroxo mixed-valent complex. On the contrary, hydroxide treatment invariably led to demetalation of the complex while addition of triethylamine gave quantitative reduction to the diferrous state as judged from electronic absorption and NMR spectroscopies.[26]

Mössbauer Spectroscopy. We recently published a Mössbauer study of diiron complexes of the asymmetrical ligand HL-BnOH (Chart 1) which provides one iron of the pair with a terminal phenolate ligand.[16] A drastic increase of the quadrupole splitting value (from 0.30 to ca. 1.0 mm/s) was noticed for the Fe^{3+} ion bound to the terminal phenolate ligand, with respect to that bound to the three nitrogen donors of the bis(picolyl) branch. This is due to the change in the asymmetry of the charge distribution introduced by the anionic ligand. It is therefore possible, using Mössbauer spectroscopy, to distinguish a complex with a neutral ligand, acetonitrile or water, from one having a hydroxo ligand. Indeed, the latter complex will exhibit a larger quadrupole splitting value compared to the former ones. Figure 7 shows the zero-field Mössbauer spectra recorded at 77 K for (A) the electrochemically oxidized acetonitrile solution of $[Fe^{III}(L\text{-}Bn)(mpdp)Fe^{II}(CH_3CN)]^{2+}$ (therefore containing $[Fe^{III}(L\text{-}Bn)(mpdp)Fe^{III}(CH_3CN)]^{3+}$) and (B) the solution obtained after water addition to the previous solution (the solid lines above the experimental spectrum correspond to its deconvolution into individual iron sites).

Spectrum A in Figure 7 is poorly resolved in the −1.0 to 1.0 mm/s range. Nevertheless, it can be fitted by considering three distinct iron sites. The first iron site (trace A1, 42(1)%) corresponds to an Fe^{3+} center with Mössbauer parameters $\delta/Fe = 0.47(1)$ mm/s and $\Delta E_Q = 0.40(1)$ mm/s, which are very close to those obtained for the Fe^{3+} center in $[Fe^{III}(L\text{-}Bn)(mpdp)Fe^{II}(CH_3CN)]^{2+}$ (Table 3 and Figure 4, trace A2). The second site (trace A2, 42(1)%) also corresponds to an Fe^{3+} center with Mössbauer parameters $\delta/Fe = 0.40(1)$ mm/s and $\Delta E_Q = 0.25(1)$ mm/s. These two sites are attributed to the $[Fe^{III}(L\text{-}Bn)(mpdp)Fe^{III}(CH_3CN)]^{3+}$ species. The additional site (trace A3, 16(1)%) is attributed to a high-spin Fe^{3+} impurity ($\delta/Fe = 0.32(1)$ mm/s and $\Delta E_Q = 0.98(1)$ mm/s), probably a degradation product of the electrochemically oxidized $[Fe^{III}(L\text{-}Bn)(mpdp)Fe^{II}(CH_3CN)]^{2+}$ complex.

After addition of water, spectrum B is obtained that extends over a larger velocity range (wings appear at −0.4 and 1.2 mm/s) and looks more complicated but better resolved than spectrum A (Figure 7). This suggests that at least one new iron species is involved in the sample. This spectrum can be fitted by considering essentially three distinct iron sites. The first iron site (trace B1, 48(1)%) corresponds to an Fe^{3+} center with $\delta/Fe = 0.48(1)$ mm/s and $\Delta E_Q = 0.44(1)$ mm/s; these parameters are close to those obtained for the Fe^{3+} centers in $[Fe^{III}(L\text{-}Bn)(mpdp)Fe^{II}(CH_3CN)]^{2+}$ and $[Fe^{III}(L\text{-}Bn)(mpdp)Fe^{III}(CH_3CN)]^{3+}$ (Table 3 and traces A2 in Figure 4 and A1 in Figure 7, respectively) and are likely to be associated with the Fe^{3+} ion in the $[N_3O_3]$ site. The second and third sites (trace B2, 26(1)%, and trace B3, 22(1)%, respectively) correspond to two Fe^{3+} centers with the same isomer shift value ($\delta/Fe = 0.55(1)$ mm/s) and quadrupole splitting values $\Delta E_Q = 0.60(1)$ and 1.51(1) mm/s, respectively. These three iron sites are proposed to be associated with two dinuclear Fe^{3+} species. Under this assumption, the second iron site is likely to be the $Fe^{3+}\text{-}OH_2$ center in the aqua complex $[Fe^{III}(L\text{-}Bn)(mpdp)Fe^{III}(H_2O)]^{3+}$ (≈52% abundance). One can notice a significant increase of the quadrupole splitting value when going from the second to the third iron site (0.60 to 1.51 mm/s). This latter feature is reminiscent of the parameters observed for the Fe^{3+} center linked to the terminal phenolate ligand in related complexes ($\delta = 0.570(5)$ mm/s and $\Delta E_Q = 0.99(2)$ mm/s for $[Fe^{II}(L\text{-}BnO)(dpp)_2Fe^{III}]^{2+}$ and $\delta = 0.550(4)$ mm/s and $\Delta E_Q = 1.220(7)$ mm/s for $[Fe^{III}(L\text{-}BnO)(dpp)_2Fe^{III}]^{+}$[16] (where dpp stands for diphenyl phosphate). Such a large quadrupole splitting is consistent with the presence of an anionic ligand on the third iron site. This anion results from water addition to the acetonitrile solution of $[Fe^{III}(L\text{-}Bn)(mpdp)Fe^{III}(CH_3CN)]^{3+}$. Therefore, it is likely to be a hydroxo ligand. We propose that the second dinuclear species (≈44%) corresponds to the $[Fe^{III}(L\text{-}Bn)(mpdp)Fe^{III}(OH)]^{2+}$ species. In addition, a high-spin Fe^{3+} impurity is present (trace B4, ≈4%). It must be noted that all attempts to increase the

number of Fe^{3+} sites did not improve significantly the fit of the spectrum shown in Figure 7. The Mössbauer parameters obtained for all iron sites in $[Fe^{III}(L\text{-}Bn)(mpdp)Fe^{III}(CH_3CN)]^{3+}$, $[Fe^{III}(L\text{-}Bn)(mpdp)Fe^{III}(H_2O)]^{3+}$, and $[Fe^{III}(L\text{-}Bn)(mpdp)Fe^{III}(OH)]^{2+}$ are summarized in Table 3.

Discussion

Acetonitrile/Water Exchange. The replacement of the acetonitrile terminally bonded to the Fe^{2+} ion by a water molecule brings a significant perturbation of the electronic structure of the diiron center which has been probed by various spectroscopic and electrochemical techniques. Indeed, electronic absorption spectroscopy reveals a 275 cm^{-1} increase in the energy of the phenolate to Fe^{III} charge-transfer transition. Such an energetic difference is small when compared to those observed for axial ligand variations in ferric salen complexes[33] or in phenolato-substituted tris(picolyl)amine complexes.[34] In the latter case, addition of excess water to the Fe^{3+} complex in acetonitrile causes an energy increase of 3850 cm^{-1} of the charge-transfer transition. This effect was attributed to the substitution of acetonitrile by water. A ca. 15 times smaller effect is observed in the present study. This is due to the fact that the coordination change occurs on the Fe^{2+} while it is observed on the phenolate to Fe^{3+} charge-transfer transition. Substitution of the weak acceptor acetonitrile by the weak donor aqua ligand will decrease the strength of the phenolate−Fe^{II} bond, thereby enabling the phenolate to engage in a stronger bond with the Fe^{3+} ion.

Owing to the intrinsic anisotropy of the Fe^{2+} ion it is difficult to analyze the changes in the NMR chemical shifts of the various protons induced by the terminal ligand exchange. Nevertheless, one observes an overall decrease of the NMR spectrum width upon going from acetonitrile to aqua ligand amounting to ca. 10% (600 to 550 ppm). Such a reduction of the spectrum width may be related to a small strengthening of the antiferromagnetic exchange interaction within the (μ-phenolato)bis(μ-carboxylato)$Fe^{II}Fe^{III}$ core. Within the theoretical framework developed by Hoffmann[35] and Kahn,[36] the magnetic exchange interaction is proportional to the overlap of the magnetic orbitals and inversally proportional to their energy splitting. The above discussion suggests that the substitution of acetonitrile by an aqua ligand will reduce the overlap between the orbitals of the phenolic oxygen and those of the Fe^{2+} ion while increasing the overlap with those of the Fe^{3+} ion, the two effects counterbalancing each other. On the other hand, it will increase the energy of the orbitals of the Fe^{2+} fragment and therefore decrease the energy gap between the magnetic orbitals. The latter effect may overcome the former leading to an increase in the antiferromagnetic exchange, but the overall effect is small.

Table 4. Electrochemical[a] Data for $[Fe^{III}(L\text{-}Bn)(mpdp)Fe^{II}(S)]^{2+}$ Complexes

complex	$E_{1/2}$(red)[b]	$E_{1/2}$(ox)[b]	ΔE (V)	K_{com}	refs
S = phenolate	−0.35	0.63	0.98	3.8×10^{16}	16
S = CH_3CN	+0.20	1.08	0.88	7.6×10^{14}	this work
S = pyridine	+0.15	0.88	0.73	2.2×10^{12}	20
S = H_2O	+0.18	0.86	0.68	3.1×10^{11}	this work

[a] Vs NHE, determined by cyclic voltammetry at 100 mV s^{-1} in CH_3CN or CH_2Cl_2 + 0.1 M TBAP at a platinum disk electrode. [b] $E_{1/2} = (E_{pa} + E_{pc})/2$, where E_{pa} and E_{pc} are the anodic and the cathodic peak potentials.

A change in the anisotropy of the Fe^{2+} ion is likely to contribute also to the narrowing of the spectrum. Indeed, the most important changes are observed in the methylenic protons of the picolyl group bound to Fe^{II}.

The electrochemical methods are able to probe both coordination sites and the diiron center as a whole. Upon replacement of acetonitrile by water, the oxidation potential decreases by 210 mV while the reduction potential decreases by 30 mV. Both the sign and the magnitude of these potential shifts are consistent with the stronger electron-donating character of the aqua ligand and its binding to the Fe^{2+} ion.

The half-wave potential difference between the oxidation (eq 2) and the reduction (eq 3) of the mixed-valent species ($\Delta E = E_{1/2}(ox) - E_{1/2}(red)$) can be related to the equilibrium constant of the comproportionation (K_{com}) reaction as follows:

$$\Delta E = (RT/nF) \ln K_{com}$$

$$[Fe^{II}(L\text{-}Bn)(mpdp)Fe^{II}(L)]^{+} + [Fe^{III}(L\text{-}Bn)(mpdp)Fe^{III}(L)]^{3+} \rightleftarrows 2[Fe^{III}(L\text{-}Bn)(mpdp)Fe^{II}(L)]^{2+} \quad (5)$$

$$L = H_2O \text{ or } CH_3CN$$

This relationship establishes that the larger the potential difference, the larger the stability domain of the mixed-valent species. Examination of Table 4 shows that (i) the stability domain of the $Fe^{III}Fe^{II}$ complexes is strongly dependent on the terminal ligand of the Fe^{2+} ion and (ii) the substitution of acetonitrile by an aqua ligand reduces the stability domain by 210 mV corresponding to a decrease of more than 3 orders of magnitude of the comproportionation constant. Gagné[37] has identified the various factors influencing the stability of mixed-valent forms of dinuclear metal compounds. These are (i) structural changes associated with the redox reactions, (ii) Coulombic interactions, (iii) magnetic exchange between the metal centers, and (iv) electronic delocalization which is expected to stabilize the mixed-valent form. In our previous study of analogous systems possessing a terminal phenolate on one iron of the pair, we showed that the asymmetry of the charge distribution was the major contributor to the stability of the mixed-valent species.[16] In this respect, it is noteworthy that K_{com} for the aqua complex is in the range observed for the mixed-valent complexes of the tetrapyridyl[19,25] and tetraimidazole[29] phenol ligands ($K_{com} \sim 10^{12}$

(33) Pyrz, J. W.; Roe, A. L.; Stern, L. J.; Que, L., Jr. *J. Am. Chem. Soc.* **1985**, *107*, 614−620.
(34) Jensen, M. P.; Lange, S. J.; Mehn, M. P.; Que, E. L.; Que, L., Jr. *J. Am. Chem. Soc.* **2003**, *125*, 2113−2128.
(35) Hay, P. J.; Thibeault, J. C.; Hoffmann, R. *J. Am. Chem. Soc.* **1975**, *97*, 4884−4899.
(36) Kahn, O.; Briat, B. *J. Chem. Soc., Faraday Trans. 2* **1976**, *72*, 268−281.
(37) Gagné, R. R.; Spiro, C. L.; Smith, T. J.; Hamann, C. A.; Thies, W. R.; Shiemke, A. K. *J. Am. Chem. Soc.* **1981**, *103*, 4073−4081.

and 10[11], respectively). This observation highlights the similarity of the electron-donating properties of H_2O and these nitrogen donors. Acetonitrile, on the other hand, differs quite substantially from these donors and contributes significantly to the asymmetry of the charge distribution. Our present Mössbauer spectroscopic studies support this interpretation. Indeed, they have shown that the quadrupole splitting is a sensitive probe of the coordination of the Fe^{2+} site. In the aqua complex $\Delta E_Q = 2.68$ mm·s^{-1}, a value close to those of the mixed-valent complexes of the symmetric tetrapyridyl ligand ($\Delta E_Q = 2.2-2.7$ mm·s^{-1}, Table 3),[19,38] where the Fe^{2+} ion is bound by a pyridine. In the acetonitrile complex $\Delta E_Q = 3.14(1)$ mm·s^{-1} in agreement with a more asymmetric electronic distribution.

Aqua Ligand Deprotonation. Electrochemical oxidation of an hydrated acetonitrile solution of $[Fe^{III}$(L-Bn)(mpdp)-$Fe^{II}(H_2O)]^{2+}$ or addition of water to $[Fe^{III}$(L-Bn)(mpdp)-$Fe^{III}(CH_3CN)]^{3+}$ lead to the formation of the same compound that we formulate as the diferric hydroxo complex $[Fe^{III}$(L-Bn)(mpdp)$Fe^{III}(OH)]^{2+}$. We have not been able so far to obtain a direct characterization of its nature, and its formulation rests on accumulated indirect but convergent evidence: (i) The overall chemical reversibility of the oxidation of $[Fe^{III}$(L-Bn)(mpdp)$Fe^{II}(H_2O)]^{2+}$ indicates that the chemical reaction following the oxidative electron transfer does not imply a drastic chemical change. (ii) The liberation of protons during the oxidation was shown. (iii) The hypsochromic shift of the electronic absorption of the oxidized solution indicates the presence of an electron donating ligand. (iv) The value of the reduction potential of the resulting diferric species matches those of complexes possessing a terminal phenolate in the same position. (v) The Mössbauer parameters of this species match those of complexes possessing a terminal phenolate, which indicates that the iron is bound by an anionic ligand. The viability of this diferric hydroxo complex $[Fe^{III}$(L-Bn)(mpdp)$Fe^{III}(H_2O)]^{2+}$ was demonstrated by reacting either the diferrous complex with *tert*-butyl hydroperoxide or **1** with *m*-chloroperbenzoic acid and analyzing the reaction mixture by electrospray ionization mass spectrometry.[39] In both cases, the dication $[Fe^{III}$(L-Bn)(mpdp)-$Fe^{III}(OH)]^{2+}$ is observed by a peak at $m/z = 438.5$, which moves to m/z 439.5 in the presence of $H_2{}^{18}O$ (Figure S3). Similar ESIMS experiments on the electrochemically oxidized solution of $[Fe^{III}$(L-Bn)(mpdp)$Fe^{II}(H_2O)]^{2+}$ could not be done owing to the presence of a large excess (at least 10-fold) of supporting electrolyte.

The observation that triethylamine does not deprotonate $[Fe^{III}$(L-Bn)(mpdp)$Fe^{II}(H_2O)]^{2+}$ but reduces it to the diferrous state is at odds with the behavior of the mononuclear Fe^{2+} complex of a poly(amino)pyridyl ligand whose aqua ligand is readily deprotonated.[40] This difference in behavior may be related to the different structures of the two complexes. Indeed, in the mononuclear compound the Fe−O(water) bond distance is exceptionally short, 1.919 Å vs 2.156 Å in $[Fe^{III}$(L-Bn)(mpdp)$Fe^{II}(H_2O)](BPh_4)_2$, where the water is trans to the phenolate.[15]

Summary and Conclusion

Combined spectroscopic and electrochemical studies have shown that the protonation state of the water-derived terminal ligand in the present diiron complexes is strongly dependent on the redox state of the iron pair. Indeed, while a hydroxide is favored for the diferric state, an aqua ligand is favored for the mixed-valent state and strictly obtained for the diferrous state. This behavior is consistent with the known deprotonation of the hydroxo bridge upon formation of oxyhemerythrin. In addition, as well the acetonitrile/water exchange as the aqua/hydroxo transformation induces a very strong perturbation of the electronic structure of the diiron center causing a change of several hundred millivolts in the redox potential values. This illustrates how deeply interrelated proton and electron transfers are in these biologically relevant diiron centers.

Supporting Information Available: Tables of X-ray crystallographic details (refined positional coordinates, anisotropic thermal parameters, complete bond lengths and angles) for complexes **1**−**3** in CIF format, temperature dependence of the χT product of $[Fe^{III}$(L-Bn)(mpdp)$Fe^{II}(H_2O)](BPh_4)_2$ (Figure S1), UV−visible spectra of the reaction of $[Fe^{III}$(L-Bn)(mpdp)$Fe^{II}(CH_3CN)]^{2+}$ with H_2O (Figure S2), and ESI-MS spectra of $[Fe^{III}$(L-Bn)(mpdp)$Fe^{III}(OH)]^{2+}$ in the absence or presence of $H_2{}^{18}O$ (Figure S3). This material is available free of charge via the Internet at http://pubs.acs.org.

IC030192+

(38) Manago, T.; Hayami, S.; Oshio, H.; Osaki, S.; Hasuyama, H.; Herber, R. H.; Maeda, Y. *J. Chem. Soc., Dalton Trans.* **1999**, 1001−1011.

(39) A 0.2 mM solution of **1** in acetonitrile is reacted at −40 °C with 4 equiv of *m*CPBA in the presence of 2000 equiv of $H_2{}^{18}O$ and the solution analyzed by ESI-MS: Avenier, F.; Dubois, L.; Latour, J.-M. Submitted for publication.

(40) Bernal, I.; Jensen, I. M.; Jensen, K. B.; McKenzie, C. J.; Toftlund, H.; Tuchagues, J. P. *J. Chem. Soc., Dalton Trans.* **1995**, 3667−3675.